

Optical Engineering

OpticalEngineering.SPIEDigitalLibrary.org

Comparison of 355-nm nanosecond and 1064-nm picosecond laser-induced damage in high-reflective coatings

Cheng Li
Yuan'an Zhao
Yun Cui
Xiaocong Peng
Chong Shan
Meiping Zhu
Jianguo Wang
Jianda Shao

SPIE

Cheng Li, Yuan'an Zhao, Yun Cui, Xiaocong Peng, Chong Shan, Meiping Zhu, Jianguo Wang, Jianda Shao, "Comparison of 355-nm nanosecond and 1064-nm picosecond laser-induced damage in high-reflective coatings," *Opt. Eng.* **57**(12), 121908 (2018), doi: 10.1117/1.OE.57.12.121908.

Comparison of 355-nm nanosecond and 1064-nm picosecond laser-induced damage in high-reflective coatings

Cheng Li,^{a,b,c} Yuan'an Zhao,^{a,b,d,*} Yun Cui,^{a,b} Xiaocong Peng,^{a,b,c} Chong Shan,^{a,b,e} Meiping Zhu,^{a,b} Jianguo Wang,^{a,b} and Jianda Shao^{a,b,*}

^aShanghai Institute of Optics and Fine Mechanics, Key Laboratory of Materials for High Power Laser, Jiading District, Shanghai, China

^bShanghai Institute of Optics and Fine Mechanics, Laboratory of Thin Film Optics, Jiading District, Shanghai, China

^cUniversity of Chinese Academy of Sciences, Beijing, China

^dChinese Academy of Sciences, Changchun Institute of Optics, Fine Mechanics and Physics, Changchun, China

^eChangchun University of Science and Technology, Changchun, China

Abstract. The damage properties of multilayer coatings tested with 1064-nm 30-ps pulses are similar to those tested with 355 nm, nanosecond pulses. A kind of HfO₂/SiO₂ high-reflective (HR) coating is prepared by electron beam evaporation. Laser-induced damage of HfO₂/SiO₂ HR coatings is tested by 355-nm 7-ns pulses and 1064-nm 30-ps pulses, respectively. Damage morphologies and cross-sectional profiles are characterized using a scanning electron microscope and focused ion beam, respectively. The laser-induced damage thresholds and morphologies in the two tests are compared. The developing processes and damage mechanisms are discussed. Many similarities are found in the two tests: the typical damage morphologies in both tests appeared as micrometer-sized pits when irradiated by low-fluence pulses, while it turned out to be layer delamination when irradiated by high-fluence pulses. Damage onset is nearby the peak of the E-field in the two tests. Damage pits in both tests may be related to thermal stress caused by nanometer-sized isolated absorbers. There are also some differences in the damage properties between two tests: damage pits in 1064-nm 30-ps tests have a much higher density than that in 355-nm 7-ns tests. The detail features and the developing processes of the pits are different. © 2018 Society of Photo-Optical Instrumentation Engineers (SPIE) [DOI: 10.1117/1.OE.57.12.121908]

Keywords: high-reflective coatings; laser-induced damage; picosecond pulse; ultraviolet-pulsed laser.

Paper 181020SS received Jul. 13, 2018; accepted for publication Nov. 9, 2018; published online Dec. 18, 2018.

1 Introduction

Laser-induced damage in optical components has always been a key challenge in the development of high-power laser systems. Different from the thermal effect induced by isolated defects in a nanosecond regime^{1,2} and electric-field-induced ionization process in femtosecond regime,^{1,3,4,5} the laser-matter interactions in the picosecond regime are quite complicated and the damage mechanism is not yet understood.

Our previous study⁶ has reported that laser-induced damage of HfO₂/SiO₂ high-reflective (HR) coatings tested with 1064-nm 30-ps pulses share similar damage morphologies to those tested with 355 ns, nanosecond pulses,⁷ which are both high-density micrometer-scale pits and nanometer-sized absorbers are inferred to be the damage initiators in both cases.⁷⁻⁹ Electron transition is one of the most common processes during laser-matter interaction, which is directly affected by photon energy and intensity of incident laser. Therefore, the comparison between damage mechanisms of 355-nm nanosecond pulses and 1064-nm picosecond pulses-induced damage in HR coatings is well worthy since there is a higher laser intensity in the former case while a greater photon energy in the latter case.

In this paper, laser-induced damage tests are carried out with 355-nm 7-ns pulses and 1064-nm 30-ps pulses, which are called as 3- ω 7-ns tests and 1- ω 30-ps tests, respectively,

when mentioned below. The damage morphologies and developing processes are compared, and the damage mechanisms are discussed.

2 Experiment

The HR coatings designed for this study have a coating stack of G|8L(0.47H0.47L)¹³(H2L)¹⁶H4L with a total thickness of 9306 nm, where G represents fused silica, H and L indicate low refractive index material (SiO₂) and high index oxide (HfO₂) with quarter wavelength optical thickness (QWOT), respectively. The QWOT for H and L layers are 103.62 and 137.94 nm, respectively. The coatings were deposited by electron beam evaporation, and the reflectivity of the coatings for S-polarized pulses and P-polarized pulses when the angle of incidence (AOI) was 45 deg as designed was 99.99% and 99.62%, respectively, at 1064 nm, 99.98% and 99.34%, respectively, at 355 nm.

355-nm damage tests were executed with the Spectra Physics Nd:YAG laser, which produces linear polarization pulses with duration of 7.8 ns at a wavelength of 355 nm at 10 Hz, single-pulse mode could be achieved by a shutter. 1064-nm damage tests were carried out with pulses generated by PL2143B Nd:YAG laser, it emits 1064-nm 30-ps pulses at a repetition rate of 10 Hz or in single-pulse mode. Both damage tests were carried out in 1-on-1 mode with S-polarized and P-polarized pulses in two AOIs of 30 deg and 50 deg, which can regulate the electric field (E-field).

*Address all correspondence to: Yuan'an Zhao, E-mail: yazhao@siom.ac.cn; Jianda Shao, E-mail: jdshao@siom.ac.cn

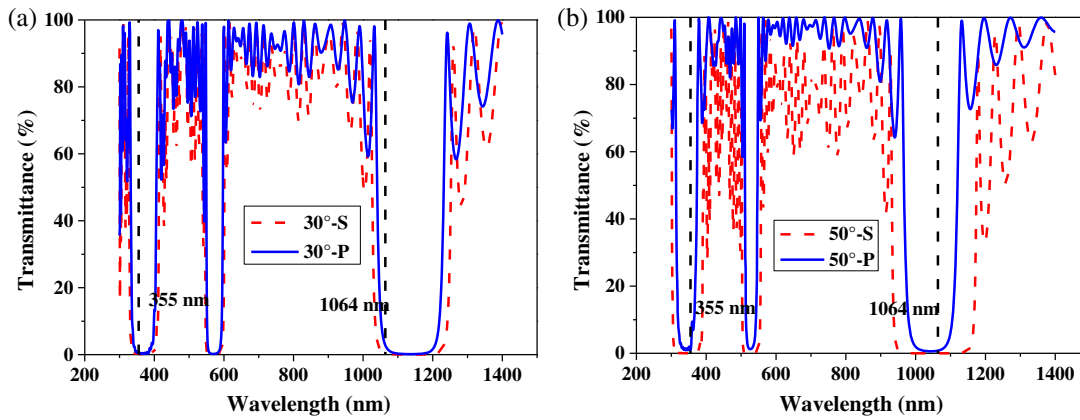


Fig. 1 The spectra of HR coatings for AOI of: (a) 30 deg and (b) 50 deg. The solid blue lines indicate P-polarization and red-dashed lines indicate S-polarization.

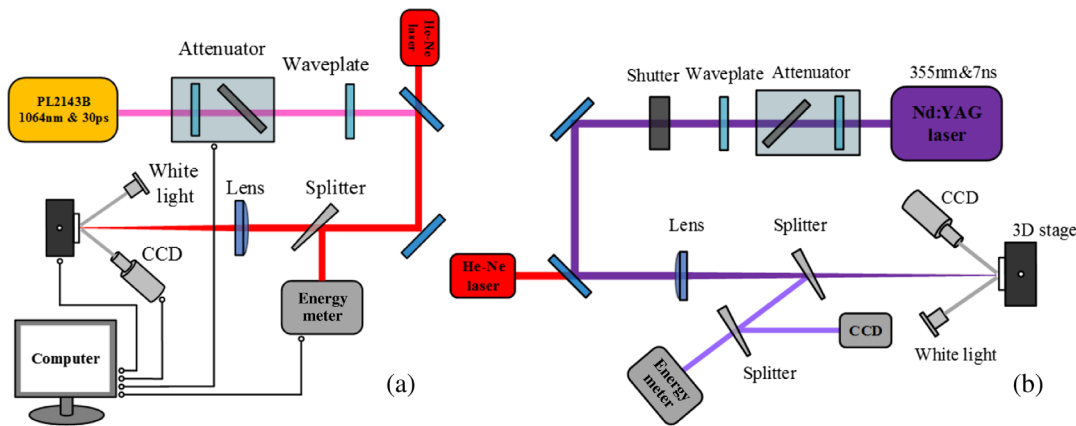


Fig. 2 Schematic figures of: (a) $1-\omega$ 30-ps tests and (b) $3-\omega$ 7-ns tests experimental setup.

In both AOIs, the reflectivity of coatings for S-polarized and P-polarized pulses at 355 nm and 1064 nm were all greater than 97.5%, as shown in Fig. 1.

The experimental setup is depicted schematically in Fig. 2. For the $1-\omega$ 30-ps tests, a $\lambda/2$ plate combined with a polarizer form an attenuator, which can adjust the laser energy by rotating the $\lambda/2$ plate. Another $\lambda/2$ plate was placed downstream from the attenuator to change the polarization. The pulse was then directed to a 96/4 beam splitter, the pulse energy was measured in the reference path with an energy meter. The samples were mounted on a motorized $x-y$ rotation stage and positioned in the focal plane of a focusing lens. The $\omega_{1/e}^2$ spot size at the focus was measured to be $180 \pm 7 \mu\text{m}$ by a laser beam profiler. The *in situ* damage detection was achieved by a CCD camera, a He-Ne laser overlapped with main path was used to assist the detecting. The samples were observed with an optical microscope after damage tests to confirm the damage. Any change in the samples after laser irradiation was regarded as damage. The setup for $3-\omega$ 7-ns tests was similar to that for $1-\omega$ 30-ps tests, an additional shutter was used to trigger the pulse in the 1-on-1 damage tests, the $\omega_{1/e}^2$ spot size was $378 \pm 10 \mu\text{m}$.

3 Results and Discussion

The laser-induced damage thresholds (LIDTs) of coatings in $1-\omega$ 30 ps tests and $3-\omega$ 7-ns tests with corresponding E-field

distributions were demonstrated in Fig. 3. The damage thresholds in this paper are all 0%-LIDTs. As seen in this figure, huge differences in the E-field can be found between two AOIs in both tests, but the LIDTs show no apparent difference. The LIDTs of the coatings should follow a τ^x scaling law when $\tau > 20$ ps if tested in the same wavelength,¹ where x ranging from 0.35 to 0.5. For our tests, the x ranged from 0.15 to 0.23 for all test conditions. The deviation of the scaling law resulted from different wavelengths in the two tests. Typical damage morphologies were shown in Figs. 4 and 5. For $1-\omega$ 30-ps test, the damage sites appear as high-density ripple-like pits with a size of several micrometers when the samples were irradiated by low-fluence pulses. In contrast, for high-laser fluences all damage morphologies appear to be layer delamination. There are also some tiny pits distribute in the low-fluence damage sites, marked in Fig. 4(b). For $3-\omega$ 7-ns test, micrometer-sized pits also shown as the typical damage morphology for low-fluence pulses, all of which are flat-pits. The density of these pits increases with higher fluence, and they will connect together, leading to a continuation of damage when the fluence get high enough. The AOIs and polarizations do not seem to have obvious influence on the damage morphology in both tests.

The cross-section images of tiny damage pits in both tests and the corresponding E-field were depicted in Figs. 6 and 7. The darker layers in the cross-section images represent silica

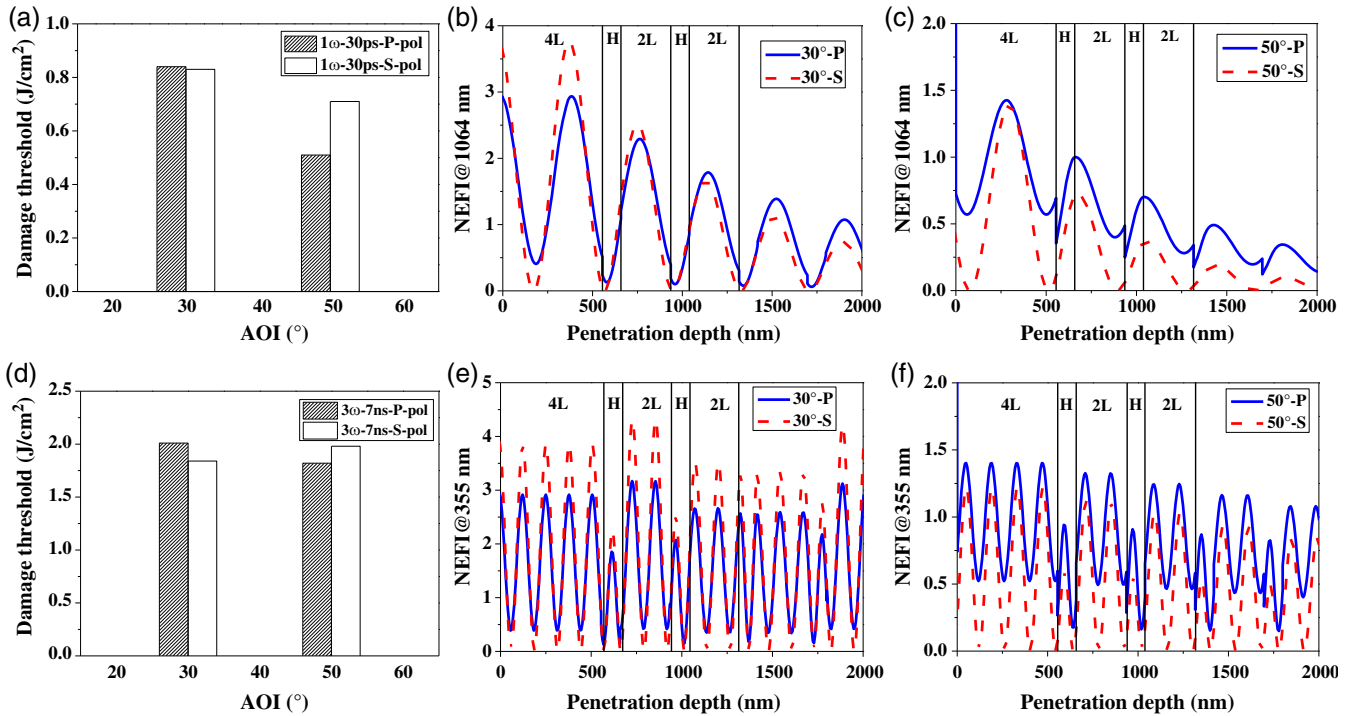


Fig. 3 The damage thresholds of coatings in: (a) 1ω 30-ps tests and (d) 3ω 7-ns tests. (b), (c) and (e), (f) The corresponding E-field, respectively.

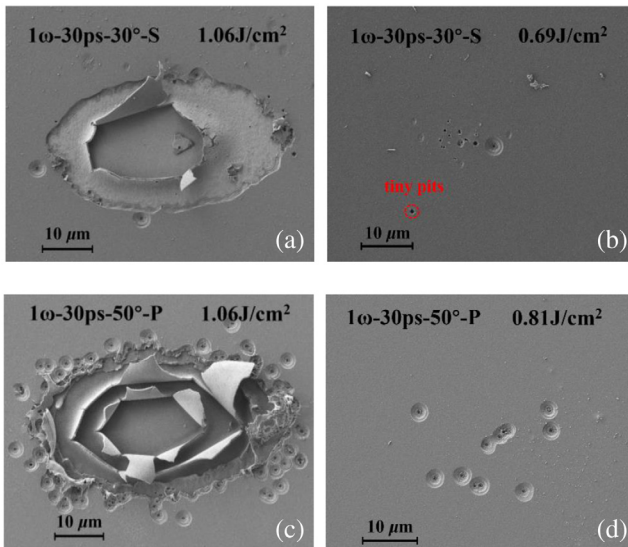


Fig. 4 Typical damage morphologies of coatings in 1ω 30-ps tests. Red circle in (b) indicates the tiny pits.

while the grey layers indicate hafnia. The influence of E-field on the damage onset can be explored by comparing it with the locations of the pits. Size and depth of the flat-pits in 3ω 7-ns tests were also characterized by atomic force microscope (AFM), which was not applicable for ripple-like pits tested by 30-ps 1064-nm pulses due to its much smaller size (2 to 4 μm). Extensive AFM tests were carried out to assist study of this issue. It can be seen in Figs. 6 and 7 that all the pits located near to the peak of corresponding E-field regardless of AOIs and polarizations, which are the 4L layer for 1ω 30-ps tests and the first 2L layer for

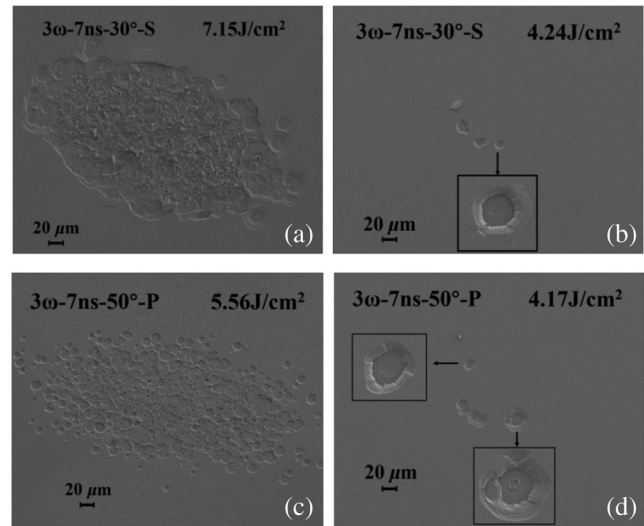


Fig. 5 Typical damage morphologies of coatings in 3ω 7-ns tests.

3ω 7-ns tests, respectively. This result is in good accordance with our previous work that the damage of HR coatings irradiated by picosecond pulses onset in the peak of E-field.⁶

Our previous study has reported similar damage morphologies for HR coatings in 1ω picosecond tests and in 3ω nanosecond tests.^{6,7} The damage in these two tests both induced by nanometer scale absorbers, hence we attempted to compare the features of damage in the two tests to explore the differences and relations of the two damage mechanisms. The damage densities were compared first and the results were demonstrated in Fig. 8. The pits density in the 1ω 30-ps tests is much higher than that in the 3ω 7-ns tests for all cases. Different pits density may indicate different

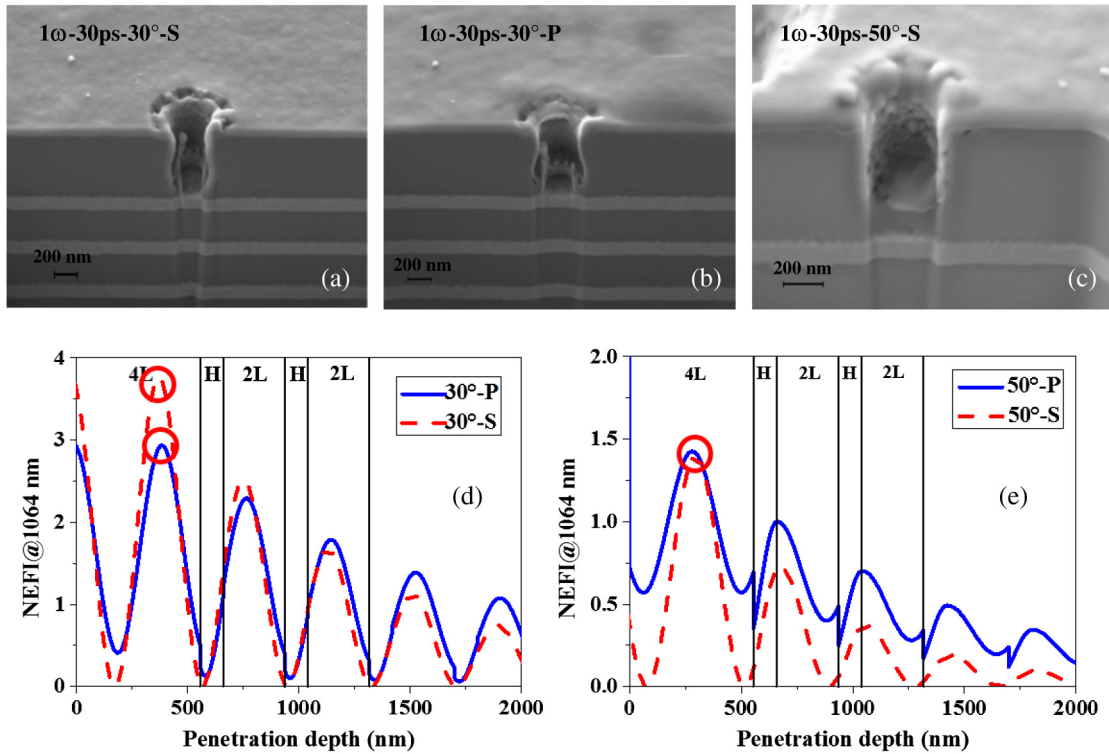


Fig. 6 (a)–(c) Cross sections of tiny pits of coatings in 1ω 30-ps tests and (d) and (e) corresponding E-field. Red circles in (d) and (e) are the approximate locations of tiny pits.

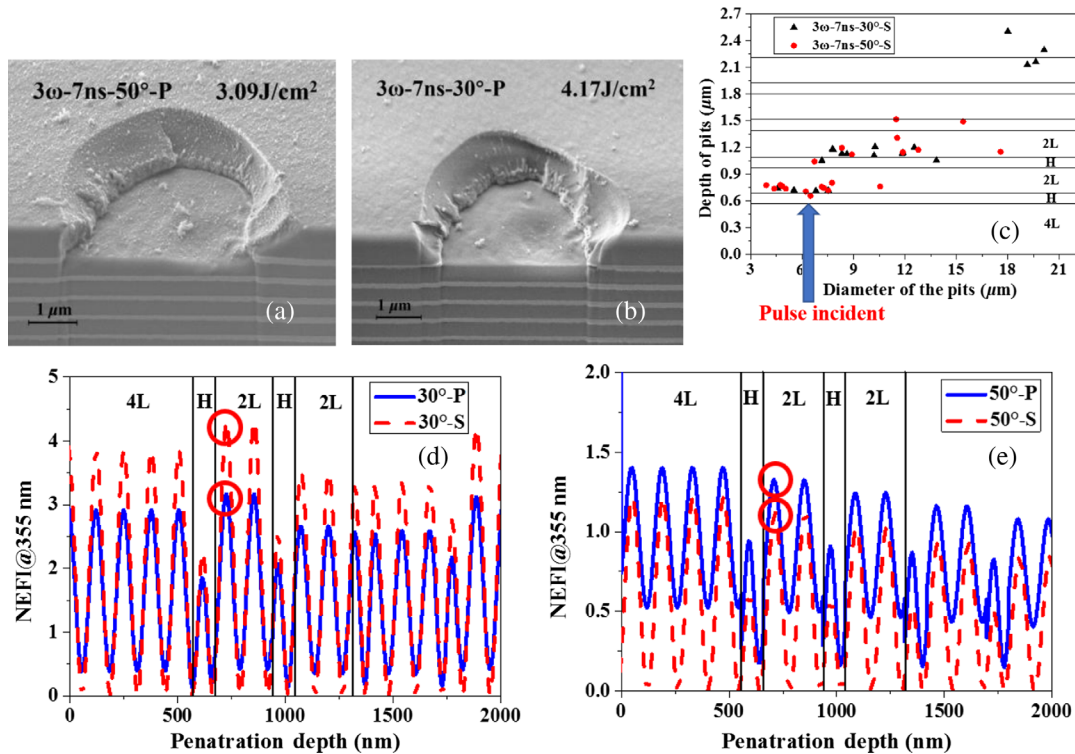


Fig. 7 (a) and (b) Cross sections of damage pits of coatings in 3ω 7-ns tests and (d) and (e) corresponding E-field. (c) The statistical data of the pits by AFM tests. Red circles in (d) and (e) are the approximate locations of damage pits.

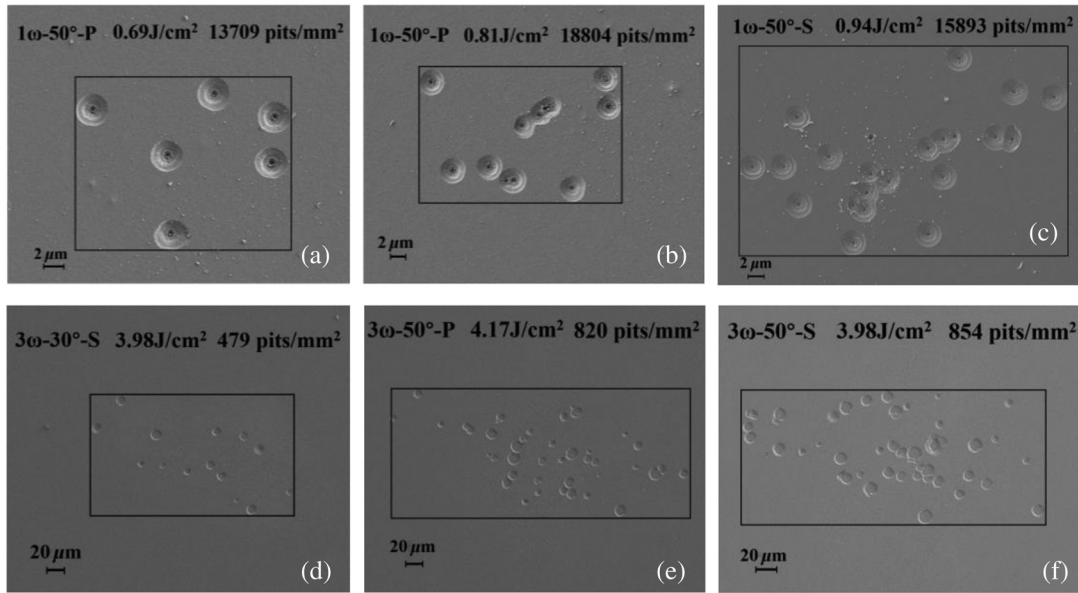


Fig. 8 Damage densities of coatings in: (a)–(c) 1- ω 30-ps tests and (d)–(f) 3- ω 7-ns tests.

damage initiators, but more evidences and analysis are needed to further research it.

Considering the different densities and the morphologies of the pits in the two tests, we set out to explore the damage mechanisms of these two tests. A mass of pits with different sizes which are more likely to represent different developmental stages in the damage process has been characterized by the focused ion beam. Figures 9 and 10 exhibited the developmental process of the pits in 1- ω and 3- ω tests, respectively. For 1- ω 30-ps test, the onset of damage causing cylindrical pits located in the 4L layer. The damaged area will be then spread out to surrounding regions in the radial direction, leading to a conical morphology, and a cylindrical pit was formed in deeper layers simultaneously, but it is still uncertain whether the damage develop into deeper layers or damage occurred somewhere deeper and then remove upper layers. Finally, ripple-like pits were formed as illustrated in

Fig. 9(d). For 3- ω 7-ns test, the damage onset is in the first several layers, forming a flat-pits, most of which located at the first L layer. Then bulge began to appear at the center of the pits, followed by the fracture of the bulge, and a deeper pit was formed, seen in Fig. 10(c). The developing process of the pits demonstrates that the damage onset deep into the layers where the absorbers distributed in, then the damage spread upward to the surface of the coatings, forming the damage pits. Due to the melting morphology in the HfO₂ layer which can be found in Figs. 10(a) and 10(b), the thermal-related process plays an important role in the damage process. For both test cases, damage onset is in the silica layers near the peak of corresponding normalized electric field intensity, therefore, the isolated precursors are more likely to locate in the silica layers.

There are some new but more interesting findings about the damage development for 1- ω 30-ps test under the

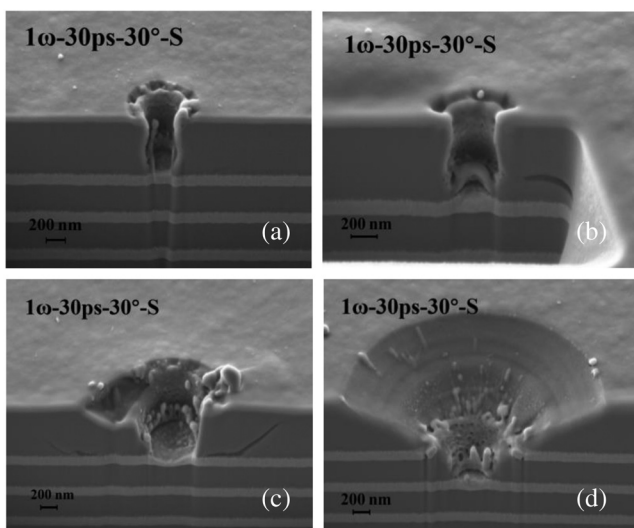


Fig. 9 (a)–(d) Cross sections of pits of coatings in different developmental stages in 1- ω 1064-ps tests.

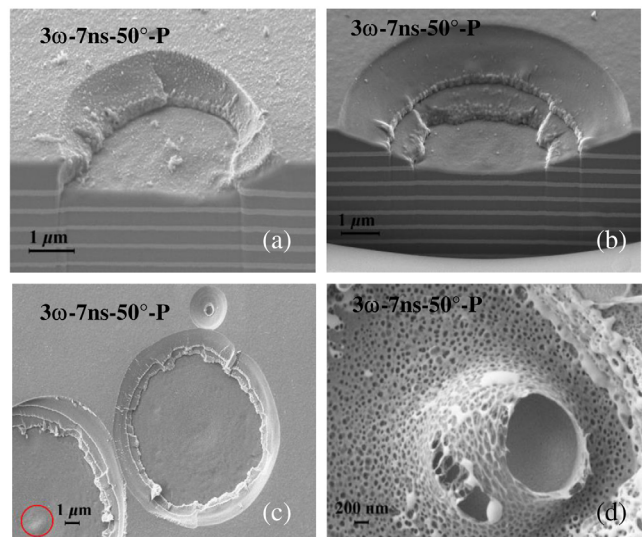


Fig. 10 (a)–(d) Cross sections of pits of coatings in different developmental stages in 3- ω 7-ns tests.

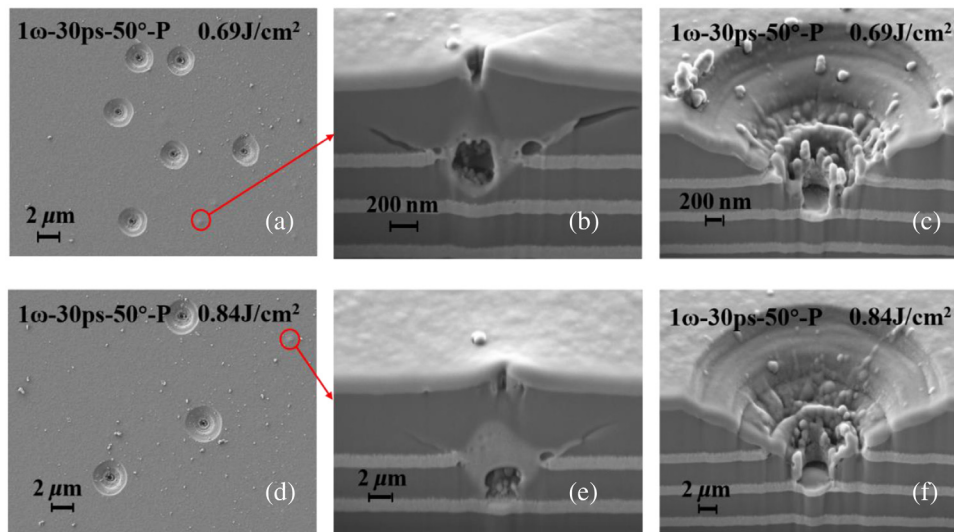


Fig. 11 (a) and (d) Damage morphologies and (b), (c), and (d)–(f) cross sections of the pits of coatings in different developmental stages, in $1-\omega$ 1064-ps tests with P-polarized pulses for AOI of 50 deg. (b) and (e) The cross sections of pits marked in red circles in (a) and (d), respectively.

circumstance of P-polarized pulses in the AOI of 50 deg. Figure 11 showed the developing process in this case. The tiny pits appeared in other test conditions depicted in Figs. 4(b), 9(a), and 9(b) can no longer be observed here, but some much more smaller pits accompanied by a tiny bulge instead, which were marked with red circles in Figs. 11(a) and 11(d). The damage initiated at the absorbing defects within the coating, which strongly absorb the laser energy, heating the vicinal materials. With the temperature rising rapidly, photoionization of the surrounding matrix occurred and formed the plasma.^{10,11} The laser energy was then absorbed successively by the plasma and the heat spread out, leading to a temperature gradient in the coatings. Cavities appeared in the process resulted from the vaporization of materials and cracks also occurred simultaneously due to thermal stress. Then, the laser energy was absorbed successively in the absorption area, heated areas expanded and a more and more stronger stress perpendicular to the sample surface teared above layers, the scalding also passing downward meanwhile, leading to ripple-like pits after recondensation of the melted material. The ripple-like pits share an almost identical morphology with that of other samples.

4 Conclusion

The laser-induced damage of $\text{HfO}_2/\text{SiO}_2$ HR coatings by $3-\omega$ 7-ns laser pulses and $1-\omega$ 30-ps laser pulses was compared. The damage properties showed something similar between two tests. When irradiated by low-fluence pulses, damage appeared as micrometer-sized pits in both tests and the morphology turned out to be layer delamination when tested with high-fluence pulses. Damage onsets are near the peak of the E-field in both test cases. Differences can also be explored between these two tests. The pits tested with $1-\omega$ 30-ps pulses have a much higher density than those with $3-\omega$ 7-ns pulses. The pits morphologies and the developing processes are also different in the two tests. The damage in both tests could be triggered by thermal stress

resulting from the absorption of laser energy by isolated absorbers. More details of the damage process are being studied.

References

1. B. C. Stuart et al., "Nanosecond-to-femtosecond laser-induced breakdown in dielectrics," *Phys. Rev. B* **53**(4), 1749–1761 (1996).
2. D. Du et al., "Laser-induced breakdown by impact ionization in SiO_2 with pulse widths from 7 ns to 150 fs," *Appl. Phys. Lett.* **64**(23), 3071–3073 (1994).
3. B. Mangote et al., "Femtosecond laser damage resistance of oxide and mixture oxide optical coatings," *Opt. Lett.* **37**(9), 1478–1480 (2012).
4. L. Sudrie et al., "Femtosecond laser-induced damage and filamentary propagation in fused silica," *Phys. Rev. Lett.* **89**(18), 186601 (2002).
5. S. S. Wellershoff et al., "The role of electron-phonon coupling in femtosecond laser damage of metals," *Appl. Phys. A* **69**(1), S99–S107 (1999).
6. C. Li et al., "Investigation on picosecond laser-induced damage in $\text{HfO}_2/\text{SiO}_2$ high-reflective coatings," *Opt. Laser Technol.* **106**, 372–377 (2018).
7. S. Papernov and A. W. Schmid, "Localized absorption effects during 351 nm, pulsed laser irradiation of dielectric multilayer thin films," *J. Appl. Phys.* **82**(11), 5422–5432 (1997).
8. C. Wei et al., "Mechanism initiated by nanoabsorber for UV nanosecond-pulse-driven damage of dielectric coatings," *Opt. Express* **16**(5), 3376–3382 (2008).
9. S. Papernov et al., "Damage behavior of HfO_2 monolayer film containing gold nanoparticles as artificial absorbing defects," *Proc. SPIE* **5991**, 59911D (2006).
10. Y. K. Danileiko, A. A. Manenkov, and V. S. Nechitailo, "The mechanism of laser-induced damage in transparent materials, caused by thermal explosion of absorbing inhomogeneities," *Quantum Electron.* **8**(1), 116–118 (1978).
11. M. F. Koldunov, A. A. Manenkov, and I. L. Pokotilo, "Theoretical analysis of the Conditions for a thermal explosion and of a photoionization instability of transparent insulators containing absorbing inclusions," *Sov. J. Quantum Electron.* **18**(3), 345–349 (1988).

Li Cheng is a doctoral candidate student at SIOM, mainly studying the nanodefects in laser-matter interactions.

Yuan'an Zhao is a professor at SIOM, whose major research includes ultrafast laser-matter interactions, femtosecond laser micro-machining, etc.

Biographies of the other authors are not available.